1521-009X/51/3/329–337$35.00
DRUG METABOLISM AND DISPOSITION

dx.doi.org/10.1124/dmd.122.001061
Drug Metab Dispos 51:329–337, March 2023

Pharmacokinetic/Pharmacodynamic Models of an Alzheimer's Drug, Donepezil, in Rats

Akiko Kiriyama, Shunsuke Kimura, and Shugo Yamashita

Department of Pharmacokinetics, Faculty of Pharmaceutical Sciences, Doshisha Women's College of Liberal Arts, Kyoto, Japan

Received August 18, 2022; accepted December 1, 2022

ABSTRACT

To investigate the relationship between the pharmacokinetics (PK) and pharmacodynamics (PD) of donepezil (Don), simultaneous examination of the PK of Don and the change in acetylcholine (ACh) in the cerebral hippocampus was analyzed using microdialysis in rats. Don plasma concentrations reached their maximum at the end of a 30-minute infusion. The maximum plasma concentrations (C_{max}s) of the major active metabolite, 6-O-desmethyl donepezil, were 9.38 and 13.3 ng/ml at 60 minutes after starting infusions at 1.25 and 2.5 mg/kg doses, respectively. The amount of ACh in the brain increased shortly after the start of the infusion and reached the maximum value at about 30 to 45 minutes, then decreased to the baseline with a slight delay from the transition of the Don concentration in plasma at a 2.5 mg/kg dose. However, the 1.25 mg/kg group showed little increase in ACh in the brain. The PK/PD models of Don, which were constructed using a general 2-compartment PK model with/without Michaelis-Menten metabolism and the suppressive effect of conversion of ACh to choline using an ordinary indirect response model, were able to effectively simulate Don's plasma and ACh profiles. The ACh profile in the cerebral hippocampus at a 1.25 mg/kg dose was effectively simulated using both constructed PK/PD models and parameters obtained at a 2.5 mg/kg dose by the PK/PD models and indicated that Don largely had no effect on ACh. When these models were used to simulate at 5 mg/kg, the Don PK were nearly linear, whereas the ACh transition had a different profile to lower doses.

SIGNIFICANCE STATEMENT

Efficacy/safety of a drug and its pharmacokinetics (PK) are closely correlated. Therefore, it is important to understand the relationship between the drug's PK and its pharmacodynamics (PD). A quantitative procedure of achieving these goals is the PK/PD analysis. We constructed the PK/PD models of donepezil in rats. These models can predict the acetylcholine-time profiles from the PK. The modeling technique is a potential therapeutic application to predict the effect when changes in the PK are caused by pathological condition and coadministered drugs.

Introduction

In recent years, the number of patients with Alzheimer's type dementia has continued to increase year on year. As a first-line drug, cholinesterase inhibitor is often used. One of the causes of Alzheimer's disease (AD) is a decrease in acetylcholine (ACh) in the brain, which results in significant damage to the cholinergic nervous system (Davies and Maloney, 1976; Whitehouse et al., 1982; Coyle et al., 1983; Gottfries, 1985; Summers et al., 1986).

Therapy of AD requires a long-term treatment primarily to slow the rate of progression (Sugimoto et al., 1999). Donepezil (Don), a treatment of AD, preferentially and strongly inhibits acetylcholinesterase in the brain and decreases the production of choline (Cho) from ACh (Yamanishi et al., 1998a; Rogers et al., 1998b; Kosasa et al., 1998), thereby suppressing the decrease in the amount of ACh in the brain that causes AD. The main side effects of Don result from its effects on the cholinergic system and include nausea, vomiting, and diarrhea (Jackson et al., 2004; Alva and Cummings, 2008). In addition, bradycardia, arrhythmia, and heart block have been reported as side effects (Tanaka et al., 2009). While coadministration of donepezil with cilostazol has been reported to be particularly effective in patients with mild dementia (Ihara et al., 2014), this drug combination has also been reported to interact with the heart (Takeuchi et al., 2016).

The metabolic pathway of Don is complex and produces many metabolites, namely hydroxylation, N-oxidation, N-dealkylated, and O-dealkylated products by cytochrome P450 (CYP) 3A4 and CYP2D6 in human liver microsomes (Cacabelos, 2007; Coin et al., 2016). It is especially known that Don is metabolized mainly into an active O-demethylated form, 6-O-desmethyl donepezil (DMDon) (Kim et al., 2021). These metabolites are further metabolized to form glucuronidation, which are then excreted into bile and urine (Matsui et. Al., 1998a, 1998b). Some of those excretions into bile result in enterohepatic circulation (Tiseo et al., 1998; Matsui et al., 1999a). The parent compound, Don, easily crosses the blood-brain barrier (BBB), and its concentration in the brain is about twice that of its concentration in plasma. On the other hand, the metabolites cannot cross the BBB and are rarely found in the brain (Matsui et al., 1999a). The pharmacokinetics (PK) of Don

This work was supported by JSPS KAKENHI Grant Number JP21K06697.

The authors declare that they do not have known competing financial interests or personal relationships that could have appeared to influence the work reported in this paper.

dx.doi.org/10.1124/dmd.122.001061.

ABBREVIATIONS: ACh, acetylcholine; AChE, acetylcholinesterase; aCSF, artificial cerebrospinal fluid; AD, Alzheimer's disease; AIC, Akaike's Information Criterion; AUC, area under the plasma concentration-time curve; BBB, blood-brain barrier; Cho, choline; CL_{tot}, total plasma clearance; C_{max}, maximum plasma concentration; CYP, cytochrome P450; D, administered dose; DMDon, 6-O-desmethyl donepezil; Don, donepezil; K_m, Michaelis-Menten constant; k_{met}, first-order metabolic rate constant; LC-MS/MS, liquid chromatography-tandem mass spectrometry; MRT, mean residence time; PEG, polyethylene glycol; PD, pharmacodynamic; PK, pharmacokinetic; $t_{1/2}$, terminal elimination half-life; V_{max}, maximum metabolic rate.

are complex and can be affected by many factors. As a result, the effects of the drug may also be affected.

In the present study, we consider the relationship between the PK of Don and DMDon, as well as Don's efficacy as ACh esterase inhibitor, using a PK/pharmacodynamic (PD) analysis in an experimental animal model in rats. Through the results of this study, the basic relationship between the PK and PD of Don was uncovered, and information on Don's efficacy when its PK changes as a result of pathologic conditions or drug interactions can be predicted.

Materials and Methods

Materials. Donepezil, DMDon, and artificial cerebrospinal fluid (aCSF) were purchased from Cayman Chemical (Ann Arbor, MI, USA), Toronto Research Chemicals (Toronto, ON, Canada), and R&D Systems, Inc. (Minneapolis, MN, USA), respectively. Acetylcholine, Cho, and polyethylene glycol (PEG) were obtained from Nacalai Tesque, Inc. (Kyoto, Japan). Acetonitrile (liquid chromatography-mass spectrometry grade) was obtained from FUJIFILM Wako Pure Chemical Corporation (Osaka, Japan). All other reagents were of analytical grade and were obtained commercially.

Standard stock solutions of donepezil and DMDon were prepared by dissolving them in methanol to a final concentration of 1.0 mg/ml.

Animal Experiments. Male Wistar rats (Shimizu Laboratory Co., Ltd., Kyoto, Japan) weighing 315 ± 26 g (9–11 weeks old) were used throughout the study. The animal experiments were performed in accordance with the Guidelines for Animal Experiments of Doshisha Women's College of Liberal Arts. The rats were housed in pairs under controlled environmental conditions and fed commercial feed pellets with free access to water.

A microdialysis guide cannula (AG-X, Eicom, Kyoto, Japan) and dummy cannula (AD-X, Eicom) were surgically implanted into the right hippocampus (Paxinos and Watson, 1998) under general anesthesia by isoflurane inhalation, followed by 2 days of recovery prior to the animal experiments described below. After the administration experiment, brain sections were collected to confirm that the guide cannula was correctly inserted into the hippocampus.

Following the 2 days of recovery from surgery, the dummy cannula was replaced with a microdialysis probe, and the aCSF solution was perfused through the probe at a flow rate of 1.5 μl/min under anesthesia by an intraperitoneal injection of urethane (1.0 g/kg). The perfusate was discarded during the first 30 minutes of perfusion and then collected at 15-minute intervals into microtubes using a Fraction Collector (EFC-82 fraction collector, Eicom) kept at 4°C using an EFR-82 electronic cooler (Eicom). After two fractions of aCSF perfusate were collected, donepezil (1.25 and 2.5 mg/kg, prepared in 0.5 ml of PEG per rat) was intravenously infused into the right femoral vein for 30 minutes at a rate of 0.5 ml/30 minutes using a variable-speed compact infusion pump (KDS100, LMS Co., Ltd. Tokyo, Japan). The perfusate was collected until 5 hours after administration. The ACh level in aCSF before Don administration ($t = 0$) was calculated from the average of these latest two collections. On the other hand, because the Cho level in aCSF gradually decreased with time, the latest Cho level before Don administration was used as the baseline level. In parallel with perfusate collections, blood samples (120 μl) were collected from the right jugular vein using a heparinized 1.0 ml syringe at 0, 10, 20, 30, 45, 60, 90, 120, 150, 180, 240, and 300 minutes after starting the infusion. All blood samples were centrifuged to obtain their plasma fractions. Plasma samples were frozen immediately after collection and stored in a freezer at -30°C until analysis. Drug concentrations in the rat plasma were measured using a liquid chromatography tandem mass spectrometry (LC-MS/MS) assay method, as described below. It was preliminarily checked that the PD effect, namely the Ach time-profile, was minimally affected by PEG infusion. Briefly, PEG solution without Don was administered to rats using the same procedure as described above, then ACh and Cho transitions in the brain were measured by microdialysis.

Quantitative Analysis. For the extraction of Don and DMDon from rat plasma, 50 μl of plasma and 2 ml of a mixture of ethyl acetate and n-hexane (3:7) were added to a 15 ml extraction glass tube. The tube was shaken for 20 minutes and then centrifuged at 3,000 rpm for 15 minutes. The organic extracts were separated by freezing the aqueous layer, followed by decanting the organic liquid into a clean glass tube. The organic liquid was evaporated using an SPD1010 SpeedVac concentrator system (Thermo Electron Corporation, Yokohama, Japan). Extraction efficiencies were found to be above 80%. The resulting residue was reconstituted by adding 50 μl of LC-MS/MS mobile phase (acetonitrile:0.1% formic acid (9:1)), of which a 30 μl aliquot was injected into the LC-MS/MS system described below. Ten calibration curve samples were prepared by adding known amounts of Don and DMDon (0.05–50 ng) to plasma from rats.

Plasma concentrations of Don and DMDon were determined using an LCMS 8050 LC/MS/MS system (Shimadzu Co., Kyoto, Japan) equipped with a Prominence High-Performance Liquid Chromatography system (Shimadzu). The high-performance liquid chromatography system consisted of two LC-20AD pumps and a SIL-20AC automatic sample injector. The flow rate of the pump was 0.2 ml/min. The analytical column was a Cosmosil $5C_{18}$-MS-II (50 mm × 2.0 mm ID; Nacalai Tesque, Inc.) and was maintained at 40°C using a CTO-20A column oven (Shimadzu). The data were loaded onto Laboratory Solutions ver. 5.91 analytical software (Shimadzu) by connecting to a CBM-20A (Shimadzu) communication bus module. Detections were performed in multiple reaction monitoring mode of the parent and selected using product ion acting in positive mode. Donepezil and DMDon were monitored using the following mass transitions by an electrospray ionization method: Don, m/z 380.5 → 91.2; DMDon, m/z 366.5 → 91.2. Linear ranges of calibration curves were between 1 and 1000 ng/ml (absolute calibration curve method, $r > 0.995$, interday variation = 5.4% of Don and 6.3% of DMDon, both at 500 ng/ml).

Collected aCSF samples were diluted by adding the same amount of LC-MS/MS mobile phase, and ACh and Cho concentrations in aCSF were determined using an LCMS 8050 LC/MS/MS system (Shimadzu). The LC-MS/MS mobile phase was a mixture of acetonitrile:0.1% formic acid (2:8) and the analytical column was a Cosmosil $5C_{18}$-PAQ (50 mm × 2.0 mm ID; Nacalai Tesque, Inc.) that was maintained at 40°C. Detections were performed in multiple reaction monitoring mode of the parent and selected using product ion acting in positive mode. ACh and Cho were monitored using the following mass transitions, m/z 146.2 → 87.2 and m/z 104.2→60.3, by an electrospray ionization method, respectively. Linear ranges of absolute calibration curves were between 0.1 and 2.0 pmol/ml (ACh) and 10 and 250 pmol/ml (Cho). Twelve calibration curve samples were prepared by adding known amounts of ACh (0.002–0.04 pmol) and Cho (0.2–5.0 pmol) to aCSF (absolute calibration curve method, $r > 0.995$, interday variation = 4.0% of ACh and 7.9% of Cho, both at 10 pmol/ml).

PK Analysis. To obtain the PK parameters, a non-compartmental PK analysis was applied to the data. The terminal elimination rate constant, k_e, of the Don concentration-time curve was determined by linear regression of at least three data points from the terminal portion of the plasma concentration-time plot. The area under the plasma concentration-time curve after intravenous (iv) infusion, area under the plasma concentration-time curve (AUC), was calculated using the linear trapezoidal rule up to the last measured plasma concentration and extrapolated to infinity using a correction term. The terminal elimination half-life ($t_{1/2}$) was determined by dividing ln2 by k_e. The area under the first moment curve after Don administration was calculated using the linear trapezoidal rule up to last measured plasma concentration and the addition of the correction term after the last measured point to infinity. The total plasma clearance (CL_{tot}) and the mean residence times (MRT) were determined by dividing the administered dose (D) by the AUC and area under the first moment curve/AUC-T_{inf}/2, respectively, where T_{inf} is the infusion period, namely 30 minutes in this study. The volume of distribution at steady state, V_{dss}, was calculated from CL_{tot}/k_e. The maximum plasma concentration (C_{max}) and its peak time were obtained from the actual measured value.

General one- and two-compartmental PK analysis was applied to the data using Phoenix 64 WinNonlin version 8.3.3.33 (Pharsight Corporation, Mountain View, CA, USA) to fit the data to models described in Fig. 1, A and B. These models have the following assumptions: first, the rate constants for the PK process, such as k_{12}, k_{21}, and k_{10}, follow first-order kinetics, and the infusion rate of Don, k_0, follows zero-order kinetics. C_t is the plasma concentration at time t, where t is the time after starting the infusion. Indexes 1–2 represent the PK compartment numbers shown in Fig. 1. V_1 is the distribution volume of the central compartment.

Furthermore, a model that incorporates the PK of active metabolites, DMDon, was considered, as shown in Fig. 1C. The metabolic process was assumed to be first-order (first-order metabolic rate constant, k_{met}) or Michaelis-Menten (maximum metabolic rate, V_{max} and Michaelis constant, K_m) kinetics. The plasma kinetics of DMDon were assumed to follow the 1-compartment model. In PK

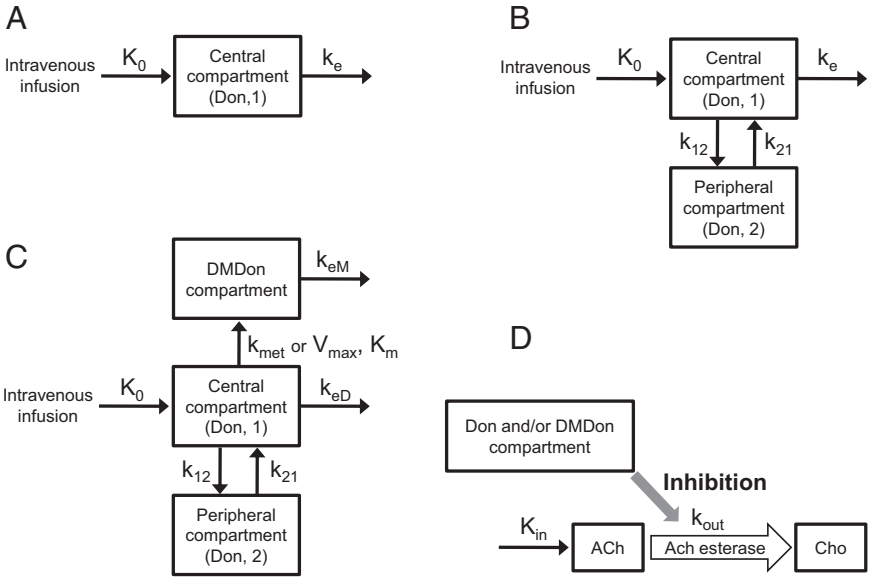

Fig. 1. Schematic representation of PK (A, B, and C) and PK/PD (D) models after Don administration (A and B); general 1- and 2-compartment model, respectively, (C); 1-/2-compartment model with either linear or Michaelis-Menten metabolism, (D); indirect-response PK/PD model for ACh changes produced by Don administration. This model is used in connection with one of Don's PK models (A, B, and C).

parameters incorporating the metabolite (DMDon) kinetics, subscripts D and M indicate Don and DMDon, respectively.

PK/PD Analysis. Figure 1D show the simple PK/PD models used in this study. Don and DMDon compartments show the PK compartments of Don and DMDon models in Fig. 1, A–C. The PK/PD parameters incorporating DMDon kinetics, subscripts D and M, also indicate Don and DMDon, respectively. All analysis were performed using Phoenix WinNonlin. The adopted PK/PD model in this study was composed of a general 2-compartmental model with/without Michaelis-Menten metabolism as a PK model and an ordinary indirect response model as a PD model. In the case of "with metabolism", the Ach esterase inhibition effect of a metabolite (DMDon) was assumed to be nearly equal to Don (Matsui et al., 1999a). In addition, the drug effect on the ordinary indirect response model is assumed to be a sigmoid E_{max} model. Using PK parameters determined from mean plasma values, PD parameters were predicted by fitting the data to the PK/PD model as related to mean PK parameters.

Assumptions of these models, in addition to the PK model, are as follows; The maximum drug effect (E_{maxD} or E_{maxM}) and the drug concentration at half-maximum effect (EC_{50D} or EC_{50M}) are constants for ordinary sigmoid E_{max} models. The γ_D and γ_M are the Hill constants. The K_{in} and k_{out} are the 0- and 1-order rate constants for ACh generation and disappearance, respectively. The average of the measured baselines at each dose was used as the initial ACh values. These values were used to calculate K_{in}/k_{out} at the model fitting. However, these concentrations in aCSF were not the actual concentration in the brain. Accordingly, these values are not directly associated with 0- and 1-order rate constants concerning ACh synthesis and disappearance in the brain.

PK/PD Simulation. Using these PK/PD parameters obtained at a 2.5 mg/kg dose and the models, namely a simple 2-compartment model without metabolic process and a 2-compartment model with Michaelis-Menten metabolism, the Don and DMDon in plasma and ACh in aCSF after 1.25, 2.5. and 5.0 mg/kg doses were simulated in 300 g rats.

Statistics. Statistical significance was evaluated by two-sided Student's *t* tests, with $P < 0.05$ considered to be statistically significant.

Results

Fig. 2 shows plasma concentration-time curves after 30-minute intravenous infusion of Don. Plasma concentrations of Don increased during infusion but had not reached a steady state. After stopping the infusion of Don, its plasma concentrations decreased. The plasma concentration profiles of DMDon are also shown in Fig. 2. DMDon is the major active metabolite of Don (Kim et al., 2021). The peak times of both doses occurred at 60–70 minutes after starting the infusion, and the C_{max} were 10.0 ± 2.8 and 13.8 ± 8.9 ng/ml after 1.25 and 2.5 mg/kg doses, respectively. These values were obtained from each measured data. When the C_{max} obtained at 2.5 mg/kg was converted into a dose of 1.25 mg/kg, it became 6.88 ± 4.47 ng/m. No significant difference was found between these values, but they tended to decrease as the dose increased. The obtained PK parameters of Don are summarized in Table 1. As the dose increased, the AUC per dose, $t_{1/2}$, and mean residence time also increased, whereas the CL_{tot} decreased. However, the V_{dss}s were almost the same.

To analyze the PK of Don, the data were adapted to several PK models described in Fig. 1. Fig. 3 shows the results. Fig. 3, A and B are the results at the 1.25 mg/kg dose and Fig. 3, C and D are those at the 2.5 mg/kg dose. Here Fig. 3, A and C are the Don plasma profile and Fig. 3, B and D are the DMDon plasma profile. The obtained PK parameters and Akaike's Information Criterion (AIC) values are shown in Table 2. The obtained data at 1.25 and 2.5 mg/kg doses were fitted to these models, and PK parameters were obtained dose-separately. As shown in Fig. 3A, in the case of 1-compartment models adapted with/without metabolism, both simulated plasma Don profiles were almost overlapped at the 1.25 mg/kg dose, and overestimation at higher plasma concentration ranges and underestimation at lower concentration ranges

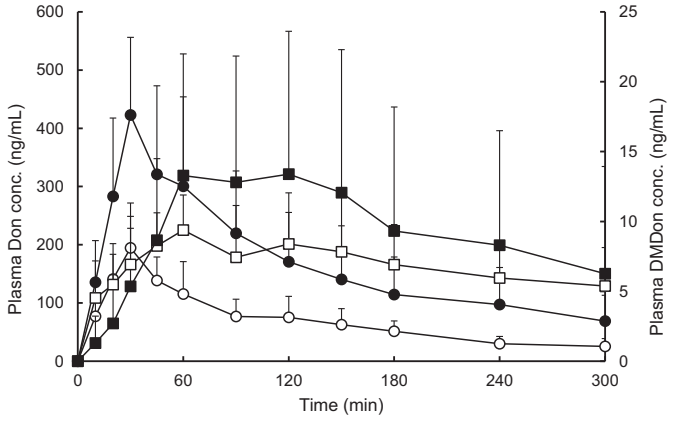

Fig. 2. Plasma concentration-time profiles of Don and DMDon after Don intravenous infusion in rats. Circles and squares represent the observed mean Don and DMDon concentrations, and closed and open symbols represent the data obtained after 2.5 and 1.25 mg/kg doses, respectively. Each point represents the mean ± S.D. of the data obtained from 7–14 experiments.

TABLE 1
Pharmacokinetic parameters of Don after intravenous infusion to rats

	PK parameters	AUC (μg×min/ml)	$t_{1/2}$ (min)	CL_{tot} (ml/min)	V_{dss} (ml)	MRT (min)
Dose	1.25 mg/kg	24.6	108	16.1	2514	148
	2.5 mg/kg	64.5	145	12.2	2562	187

Each value was calculated using the mean data obtained from 7–14 experiments.

was observed. On the other hand, plasma Don profiles at the 2.5 mg/kg dose were largely similar except for the 2-compartment model with linear metabolism, as shown in Fig. 3C. It is considered that the 2-compartment model with Michaelis-Menten metabolism showed the best fit for the overall concentration range. Examining the metabolite concentration profiles (Fig. 3, B and D), 2-compartment models with both metabolism processes at the 1.25 mg/kg dose and PK models with Michaelis-Menten metabolism at the 2.5 mg/kg dose were found to fit better. The number of data were not enough compared with the number of parameters required for model fitting. The AIC values were smaller in the 2-compartment model compared with the 1-compartment model under an identical metabolic condition. Comparing the AICs obtained between doses under the same models, the general 2-compartment model without metabolism and the 2-compartment model with Michaelis-Menten metabolism were considered to be suitable for PK analysis.

Figure 4 shows the ACh (A) and Cho (B) time profiles in aCSF at two doses. Cho was hardly affected at both Don doses and PEG administration (control). After the 1.25 mg/kg dose and in the control group, the ACh profile was also hardly affected by Don administration. The initial ACh and Cho concentrations in aCSF were 0.239 ± 0.162 and 216 ± 153 pmol/ml for the control group, 0.393 ± 0.289 and 129 ± 112 pmol/ml at the 1.25 mg/kg dose, and 0.411 ± 0.293 and 203 ± 161 pmol/ml at the 2.5 mg/kg dose, respectively. The peak time of ACh after the 2.5 mg/kg dose was between 30 and 45 minutes, although the width of the SD was relatively large. Based on these results, the ACh transition was adopted as the indicator of the effect, and PK/PD analysis was performed. In this figure, the fitting of ACh concentration profiles in aCSF is also shown. For PK/PD analysis, the ordinary 2-compartment models and that with Michaelis-Menten metabolism, as previously described, were employed as PK models, and an ordinary indirect response model was adapted as a PD model. The results revealed that the two models showed almost overlapping fitting at each dose. The calculated PD parameters are shown in Table 3. The calculated parameters are relatively similar between doses except for some EC_{50} and E_{max} values. Since an effect of Don was hardly observed at the 1.25 mg/kg dose, the obtained parameters at the 2.5 mg/kg dose were more reliable than those obtained at the low dose. The AIC values of the PK model with Michaelis-Menten metabolism are smaller than those of simple 2-compartment model at both doses. Moreover, both data sets at 1.25 and 2.5 mg/kg were tried to fit simultaneously to these two PK/PD models. The obtained PK/PD parameters were also listed in Tables 2 and 3.

Using PK/PD parameters obtained at the 2.5 mg/kg dose listed in Table 4 and two 2-compartment models (without metabolic process and with Michaelis-Menten metabolism), the Don (A) and DMDon (B) in plasma and ACh (C) in aCSF at 1.25, 2.5, and 5.0 mg/kg doses were simulated (Fig. 5). After 2.5 mg/kg dosing, the ACh concentration in aCSF was observed to be clearly increasing. Plasma Don profiles were relatively similar between models. As shown in Fig. 5B, the peak times of DMDon were all 94 minutes after administration, and the C_{max} were slightly decreased

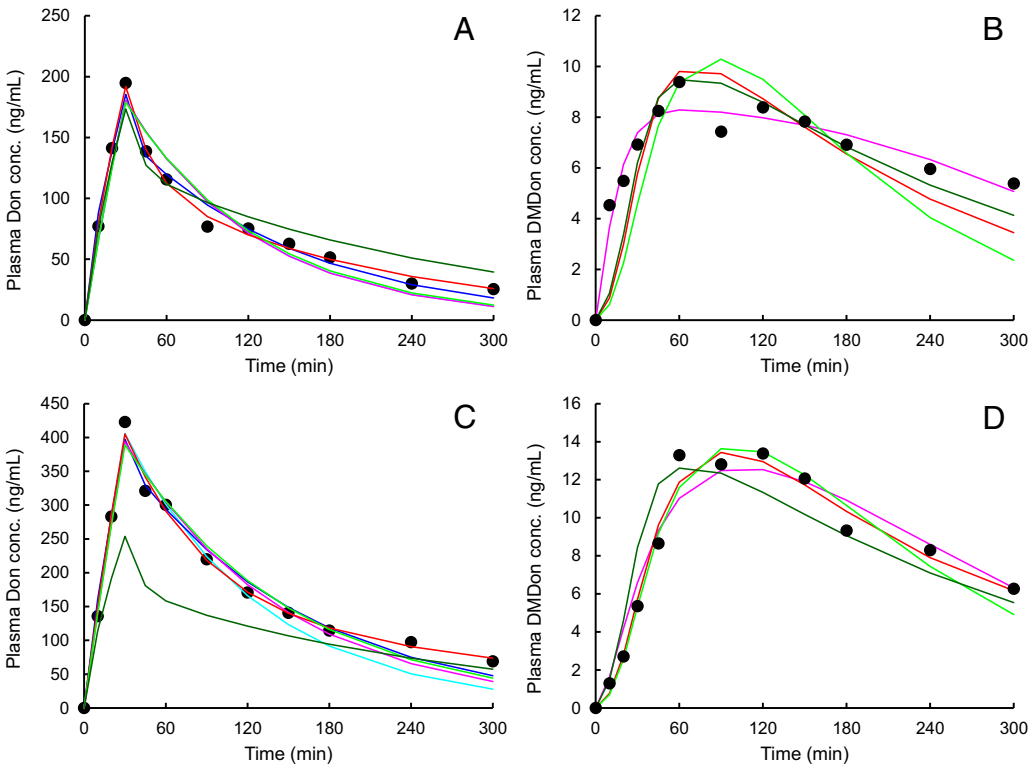

Fig. 3. Observed and fitted plasma concentrations of Don and DMDon by PK models after intravenous infusion in rats (A) and (B) are concentration profiles of Don and DMDon at the 1.25 mg/kg dose. (C) and (D) are concentration profiles of Don DMDon at the 2.5 mg/kg dose. Closed circles represent the mean values of the data Lines, (aqua); general 1-compartment model, (blue); general 2-compartment model, (pink); 1-compartment model with Michaelis-Menten metabolism, (red); 2-compartment model with Michaelis-Menten metabolism, (yellow-green); 1-compartment model with linear metabolism, (green); 2-compartment model with linear metabolism.

TABLE 2

Pharmacokinetic parameters of Don to rats calculated by several PK models shown in Fig. 1 A–C

			1-Compartment model						2-Compartment model				
			1.25 mg/kg		2.5 mg/kg				1.25 mg/kg		2.5 mg/kg		Simultaneous
Basic pharmacokinetic model of Don	Parameters		Estimate	CV (%)	Estimate	CV (%)	Parameters		Estimate	CV (%)	Estimate	CV (%)	Estimate
Compartment model	V_1	(ml)	1888	5.9	1680	4.3	V_1	(ml)	204	10.5[c]	448	90.1[b]	366
	k_e	(min^{-1})	0.0103	11.9	0.00994	8.4	k_e	(min^{-1})	0.0854	10.5[c]	0.0319	90.1[b]	0.0397
	AIC		101.9		115.0		k_{12}	(min^{-1})	1.49	12.7[c]	1.19	14.6[c]	0.970
							k_{21}	(min^{-1})	0.159	10.2[b]	0.377	27.6[b]	0.192
							AIC		92.2		109.8		192.8
Compartment model with linear metabolism	V_D	(ml)	1912	5.7	1800	3.3	V_D	(ml)	1355	34.8	1769	3485	
	V_M	(ml)	16.9	53.0[c]	0.0160	13.2[c]	V_M	(ml)	0.00476	54.8[c]	0.00468	14.3[d]	
	k_{met}	($\times 10^6$, min^{-1})	17.4	53.0[c]	0.00918	13.2[c]	k_{met}	($\times 10^6$, min^{-1})	0.0101	54.8[c]	0.0138	14.3[d]	
	k_{eD}	(min^{-1})	0.00989	93.1[a]	0.00807	15.4	k_{eD}	(min^{-1})	0.00891	60.6	0.00903	3456	
	k_{eM}	(min^{-1})	0.0195	52.5	0.0165	17.1	k_{eM}	(min^{-1})	0.0316	31.5	0.0315	22.9	
	AIC		162.1		147.7		k_{12}	(min^{-1})	0.0494	126.3	1.36	5220	
							k_{21}	(min^{-1})	0.0491	84.7	0.325	912	
							AIC		157.8		534.0		
Compartment model with Michaelis-Menten metabolism	V_D	(ml)	1885	5.8	1769	3.8	V_D	(ml)	1414	4.3	1636	3.0	1625
	V_M	(ml)	0.899	47.1[a]	0.00146	23.1[d]	V_M	($\times 10^4$, ml)	0.0853	17.9[d]	0.109	28.4[c]	0.0468
	V_{max}	(ng/ml/min)	0.646	47.0[a]	0.000757	23.1[d]	V_{max}	(ng/ml/min)	0.00283	47.8[d]	0.00222	17.2[d]	0.0290
	K_m	(ng/ml)	9.65	48.3	118	56.5	K_m	(ng/ml)	148749	83.6[a]	193951	18.5[a]	130
	k_{eD}	(min^{-1})	0.0103	21.1	0.00854	36.5	k_{eD}	(min^{-1})	0.0110	7.3	0.00627	35.0	0.00841
	k_{eM}	(min^{-1})	0.0805	15.1	0.0261	17.6	k_{eM}	(min^{-1})	0.0221	52.7	0.0164	18.0	0.0299
	AIC		132.1		154.6		k_{12}	(min^{-1})	0.0211	20.1	0.00611	22.7	0.00884
							k_{21}	(min^{-1})	0.0265	21.6	0.00703	86.9	0.0171
							AIC		132.3		132.8		275.3

CV, coefficient of variation; k_e, terminal elimination rate constant; k_{eD} and k_{eM}, first-order elimination rate constant; V_D and V_M volume distribution volume of the central compartment;
[a] $\times 10^3$.
[b] $\times 10^5$.
[c] $\times 10^6$.
[d] $\times 10^7$.
Each value was calculated using the mean data obtained from 7–14 experiments.
"Simultaneous" was obtained when both data sets at 1.25 and 2.5 mg/kg were fitted simultaneously to these two PK models.

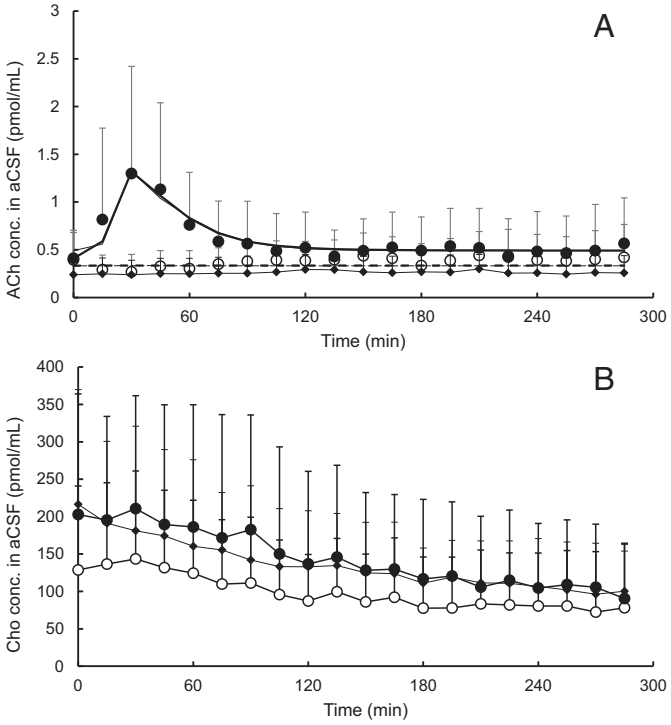

Fig. 4. Pharmacodynamic responses (ACh (A) and Cho (B) changes in aCSF) with respect to time after intravenous infusion of Don to rats. Closed and open circles represent the data obtained after 2.5 and 1.25 mg/kg doses, respectively. The closed diamond represents the data of control group (PEG solution without Don was administered). Each point represents the mean ± S.D. of the data obtained from 7–10 experiments. Fitted curves were obtained both according to the 2-compartment PK model with Michaelis-Menten metabolism (bold lines) and without (fine lines) metabolism, namely a general 2-compartment model. Solid and dashed lines represent the fitted curves at 2.5 and 1.25 mg/kg doses, respectively.

with the dose increase. Despite the PK profiles of Don being similar between the models in a dose-independent manner, ACh concentration-time curves were dose-dependent and different between models, especially at the high dose of 5.0 mg/kg.

Discussion

The PK of a drug and its effects/side effects are closely related. Therefore, plasma concentrations are measured as an index of its effect. However, the two are not in a simple proportional relationship, and many factors are involved. Therefore, PK/PD analyses were employed to explain the effects of drugs in relation to their PK (Kobuchi et al., 2014; Kiriyama et al., 2016; Kiriyama et al., 2017; Motoki et al., 2019; Kobuchi et al., 2020).

It is preferable that the PK model candidate has the required conditions/processes and is simple. In this study, the PK parameters calculated from mean plasma profiles were adopted to PK/PD models to fit PDs more exactly. In the case of Don, two models were selected to represent the PKs of Don, and in some cases DMDon. Considering the AIC and the similarity of the model fit PK parameters between doses, the following two 2-compartment models were selected to use for PK/PD analysis. One was a common 2-compartment model of Don only, and the other was a 2-compartment model with Michaelis-Menten metabolism to DMDon. As the plasma DMDon level and metabolic CL calculated by V_{max}/K_m is extremely small compared with CL_{tot}, the 2-compartment model with or without nonlinear metabolism was considered to have little effect on the PK of Don at these dose ranges. The V_{max}/K_m values calculated to be 1.91×10^{-8} and 1.14×10^{-8} min^{-1} were similar to the k_e values obtained with the 2-compartment model with linear metabolism at 1.25 and 2.5 mg/kg doses, respectively. However, when the dose increased, the DMDon time-profile changed depending on whether the metabolic process is linear or saturable.

As shown in Fig. 5, simulated Don, DMDon, and ACh concentration-time profiles after these doses were largely similar between the two models. The profile of the ACh concentration at the 1.25 mg/kg dose was effectively simulated using PK/PD parameters obtained at the 2.5 mg/kg dose by both models. Namely, the effect of Don on ACh was hardly observed at the 1.25 mg/kg dose. However, when the dose was increased to 5.0 mg/kg, the ACh concentration profiles differed in both shape and degree compared with the other two doses, and different profiles were observed between the models. The nonlinear processes in both metabolisms were considered to affect the ACh profiles. Although the data are not shown, the same PK experiments were actually performed at the 5.0 mg/kg dose. However, around 30 minutes after starting the infusion, when the highest plasma Don concentration was reached, nearly half of all rats died, likely due to cardiovascular problems. Therefore, both models could not be validated at a dose of 5.0 mg/kg.

The plasma concentration of the metabolite was one-thirtieth compared with that of the parent compound. Fourteen metabolites of Don have been reported with Don mainly metabolized to the O-demethylated form (Matsui et al., 1999a). The parent compound, Don, easily crosses the BBB, and its concentration in the brain is about twice that in plasma. On the other hand, these metabolites cannot pass through the BBB and are rarely found in the brain. The distributions of Don and DMDon into the brain were studied using rats. After oral administration of ^{14}C-labeled Don, the plasma time profile of Don decreased more rapidly than that of radioactivity in plasma. On the other hand, the radioactivity in the brain decreased almost in parallel with the plasma profile of Don. Most radioactivity in the brain is due to Don and low permeability of the metabolites through the BBB. Similar results have been obtained in experiments with dogs. More than 80% of the radioactivity in the brain was derived from Don (Matsui et al., 1998a). Therefore, it is considered that the effect of DMDon in the brain contributes minimally to its efficacy in vivo. Cholinesterase includes AChE and butyrylcholinesterase, and Don is known to selectively inhibit AChE. It has been reported that the brain contains more AChE than butyrylcholinesterase, and that the activity of Don in the brain is more potent than that in plasma, because of the difference in the type of cholinesterase (Yamanishi et al., 1998a, 1998b).

Don is readily distributed to the heart, brain, and adrenal gland in addition to the elimination tissue, liver, in rats (Watabe et al., 2014). The Don concentration-time profiles of these tissues are similar to that in plasma after intravenous administration. When Don is orally administered to rats, nearly 100% absorption is obtained, and the maximum plasma concentration is rapidly reached around 30 minutes after administration. (Matsui et al., 1998b). Our result is also supported by Kosasa et al. (Kosasa et al., 1999), who reported that orally administered Don was absorbed rapidly, leading to a rapid increase in ACh in the cerebral cortex, and the minimum effective dose of Don was 2.5 mg/kg and under in rats.

According to a report by Rogers et al., the plasma Don concentration after oral administration in humans was proportional to the dose at a low dose to a clinical dose (2.0–6.0 mg), and the clearance was almost constant regardless of the dose (Rogers and Friedhoff, 1998a). As reported, the maximum plasma concentration is reached in about 4 hours, and the $t_{1/2}$ in about 80 hours. The AChE inhibitory activity is proportional to the plasma concentration as in the results in rats. This tendency did not change in the case of repeated administration (Rogers et al., 1998b). It takes about 14 days to reach a steady state due to the long $t_{1/2}$. The

TABLE 3

Pharmacodynamic parameters of Don to rats, calculated by models shown in Fig. 1 D

Pharmacokinetic model of Don	Parameters		Dose: 1.25 mg/kg Estimate	1.25 mg/kg CV (%)	2.5 mg/kg Estimate	2.5 mg/kg CV (%)	Simultaneous Estimate
2-compartment model with Michaelis-Menten metabolism	K_{in}	(pmol/ml/min)	15.9	NA	20.1	NA	23.2
	k_{out}	(min^{-1})	47.6	NA	48.9	NA	66.7
	E_{maxD}	(pmol/ml/min)	1.20	NA	1.18	NA	1.47
	EC_{50D}	(ng/ml)	711	NA	274	NA	211
	γD		6.80	NA	5.36	NA	4.75
	E_{maxM}	(pmol/ml/min)	0.000952	NA	0.331	NA	0.0809
	EC_{50M}	($\times 10^7$, ng/ml)	2.83	NA	1.79	NA	1.59
	γM		0.627	NA	0.543	NA	0.417
	AIC		−96.1		−28.6		−45.9
2-compartment model	K_{in}	(pmol/ml/min)	9.45	17.8	26.2	29.7	25.8
	k_{out}	(min^{-1})	28.2	17.8	53.4	29.7	74.7
	E_{max}	(pmol/ml/min)	0.355	46.7	0.677	7.4	0.895
	EC_{50}	(ng/ml)	388	46.8	276	4.4	219
	γ		10.8	49.6	7.04	26.7	3.20
	AIC		−106.1		−33.5		−54.5

CV, coefficient of variation; K_{in} and k_{out}, 0- and 1-order rate constants concerning ACh generation and disappearance, respectively; NA, not available.
Each value was calculated using the mean data obtained from 7–14 experiments.
PK parameters employed in the PK/PD analysis were listed in Table 2.
"Simultaneous" was obtained when both data sets at 1.25 and 2.5 mg/kg were tried to fit simultaneously to these two PK/PD models.

accumulation rate at the repeated administration was calculated from the PK parameters obtained at a single administration. The results are largely in agreement with the observed values. Disappearance from the body is very slow and differs between rats and humans. In addition, the $t_{1/2}$ of Don in dogs is reported to be similar to that in rats. One of the factors contributing to this result is the difference in hepatic metabolic activity between these species. The hepatic CL, calculated using the well-stirred model and in vitro enzyme kinetic data, in rats and dogs is 14.4 and 7.4 times larger than that in humans, respectively (Matsui et al., 1999b). In addition, plasma protein binding of Don was slightly higher in humans compared with rats and dogs (88% versus both 74%) (Matsui et al., 1999b). Don is reported to be metabolized by CYP2D6 and CYP3A4 and is known to be metabolized into DMDon by CYP2D6 (Matsui et al., 2000). However, many CYP2D6 and CYP3A4 inhibitors do not affect Don's PK in AD patients (Prvulovic and Schneider, 2014). The relationship between the AUC and the AChE inhibitory activity after repeated administration was almost linear ($r^2 = 0.919$). Since the plasma concentration was correlated with the AChE inhibitory activity and no hysteresis was observed, the effect gradually increased as the plasma concentration increased toward the steady state. From these reports, plasma Don concentration is considered to be important for ACh profiles in the brain.

According to a report on the pharmacology of Don, the cognitive effects of Don in the pathologic brain may be elicited by both cholinergic and sigma-1 agonistic modes of action. The affinity of Don to sigma-1 receptors is similar to that of AChE (Kato et al., 1999). The cortical sigma-1 receptor density was reduced by 44–60% in AD, but not in physiologic aging (Mishina et al., 2008; Ishii et al., 2002). Don binds to this receptor with >60–70% occupation in the human brain (Ishikawa et al., 2009). Sigma-1 activation may have an important role in neuroprotection and restoration of cognitive performance in pathologic brain conditions (Hayashi and Su, 2005; Hayashi and Su, 2007; Yang S et al., 2007; Tchedre and Yorio, 2008; van Waarde et al., 2011). However, only minimal effects have been found in animals.

Interestingly, the PK model after oral administration in humans was reported to be optimal for the saturated Michaelis-Menten type with a hepatic first-pass effect and hepatic metabolism (Yoon et al., 2020). In this study, they were examining the optimal dosing schedules of Don's patch regimen in comparison with an oral regimen using the constructed PK model including Michaelis-Menten metabolism. Although there are differences in metabolic activity between humans and rats, this is consistent with our optimal model after intravenous administration. However, there are various species differences in PK and PD between rats

TABLE 4

PK/PD parameters of Don using simulations in rats

Basic pharmacokinetic model of Don	PK parameters			PD parameters		
2-compartment model with Michaelis-Menten metabolism	V_D	(ml)	1636	K_{in}	(pmol/ml/min)	20.1
	V_M	($\times 10^4$, ml)	0.109	k_{out}	(min^{-1})	48.9
	V_{max}	(ng//ml/min)	0.00222	E_{maxD}	(pmol/ml/min)	1.18
	K_m	(ng/ml)	193951	EC_{50D}	(ng/ml)	274
	k_{eD}	(min^{-1})	0.00627	γ_D		5.36
	k_{eM}	(min^{-1})	0.0164	E_{maxM}	(pmol/ml/min)	0.331
	k_{12}	(min^{-1})	0.00611	EC_{50M}	($\times 10^7$, ng/ml)	1.79
	k_{21}	(min^{-1})	0.00703	γ_M		0.543
2-compartment model	V_1	(mL)	448	K_{in}	(pmol/ml/min)	26.2
	k_e	(min^{-1})	0.0319	k_{out}	(min^{-1})	53.4
	k_{12}	(min^{-1})	1.19	E_{max}	(pmol/ml/min)	0.677
	k_{21}	(min^{-1})	0.377	EC_{50}	(ng/ml)	276
				γ		7.04

The simulations were performed with a rat weighing 300 g.

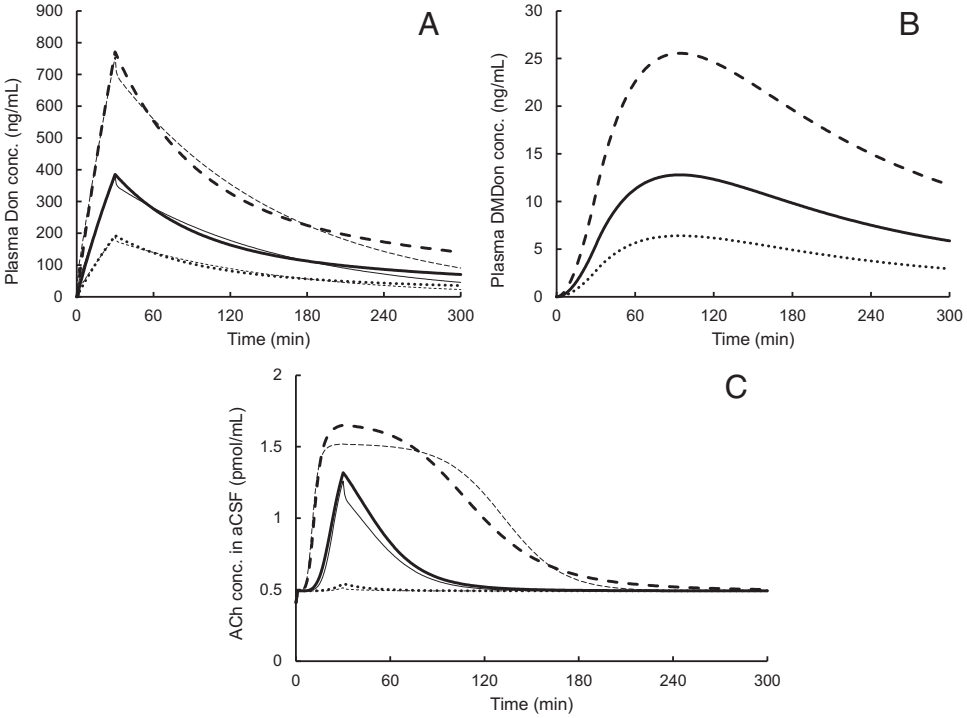

Fig. 5. Simulated profiles of Don (A), DMDon (B), and ACh (C) after Don administration in rats. The Don doses were 1.25 (dotted line), 2.5 (solid line), and 5.0 (dashed line) mg/kg. Bold and fine simulated lines (A and C) were obtained by a 2-compartment model with Michaelis-Menten metabolism and a 2-compartment model without metabolism (general 2-compartment model), respectively.

and humans. Therefore, although the PK of Don differs between humans and rats and the results of this study cannot be applied to humans, basic information for applying them to humans was obtained and this report will provide important information for PK/PD analysis in humans.

Conclusion

The PK/PD models of Don constructed using a general 2-compartment PK model with/without Michealis-Menten metabolism and an indirect ordinary response model of suppressive effect of conversion of ACh to Cho were able to effectively simulate Don's plasma and ACh profiles. Through such PK/PD model analysis, it will be possible to predict Don's PK and effects in humans from the results of animal experiments, and to estimate PK variations and drug–drug interactions.

Authorship Contributions

Participated in research design: Kiriyama.
Conducted experiments: Kiriyama, Kimura, and Yamashita.
Performed data analysis: Kiriyama, Kimura, and Yamashita.
Wrote or contributed to the writing of the manuscript: Kiriyama.

References

Alva G and Cummings JL (2008) Relative tolerability of Alzheimer's disease treatments. *Psychiatry (Edgmont)* **5**:27–36.

Cacabelos R (2007) Donepezil in Alzheimer's disease: From conventional trials to pharmacogenetics. *Neuropsychiatr Dis Treat* **3**:303–333.

Coin A, Pamio MV, Alexopoulos C, Granziera S, Groppa F, de Rosa G, Girardi A, Sergi G, Manzato E, and Padrini R (2016) Donepezil plasma concentrations, CYP2D6 and CYP3A4 phenotypes, and cognitive outcome in Alzheimer's disease. *Eur J Clin Pharmacol* **72**:711–717.

Coyle JT, Price DL, and DeLong MR (1983) Alzheimer's disease: a disorder of cortical cholinergic innervation. *Science* **219**:1184–1190.

Davies P and Maloney AJ (1976) Selective loss of central cholinergic neurons in Alzheimer's disease. *Lancet* **2**:1403.

Gottfries CG (1985) Alzheimer's disease and senile dementia: biochemical characteristics and aspects of treatment. *Psychopharmacology (Berl)* **86**:245–252.

Hayashi T and Su T (2005) The sigma receptor: evolution of the concept in neuropsychopharmacology. *Curr Neuropharmacol* **3**:267–280.

Hayashi T and Su TP (2007) Sigma-1 receptor chaperones at the ER-mitochondrion interface regulate Ca(2+) signaling and cell survival. *Cell* **131**:596–610.

Ihara M, Nishino M, Taguchi A, Yamamoto Y, Hattori Y, Saito S, Takahashi Y, Tsuji M, Kasahara Y, Takata Y et al. (2014) Cilostazol add-on therapy in patients with mild dementia receiving donepezil: a retrospective study. *PLoS One* **9**:e89516.

Ishii K, Kimura Y, Kawamura K, Sasaki T, and Ishiwata K (2002) Mapping of sigma(1) receptors by C-11-SA4503-distribution and aging effect in normal human brain. *Neuroimage* **16**:S31.

Ishikawa M, Sakata M, Ishii K, Kimura Y, Oda K, Toyohara J, Wu J, Ishiwata K, Iyo M, and Hashimoto K (2009) High occupancy of sigma1 receptors in the human brain after single oral administration of donepezil: a positron emission tomography study using [11C]SA4503. *Int J Neuropsychopharmacol* **12**:1127–1131.

Jackson S, Ham RJ, and Wilkinson D (2004) The safety and tolerability of donepezil in patients with Alzheimer's disease. *Br J Clin Pharmacol* **58**(Suppl 1)1–8.

Kato K, Hayako H, Ishihara Y, Marui S, Iwane M, and Miyamoto M (1999) TAK-147, an acetylcholinesterase inhibitor, increases choline acetyltransferase activity in cultured rat septal cholinergic neurons. *Neurosci Lett* **260**:5–8.

Kim SE, Seo HJ, Jeong Y, Lee GM, Ji SB, Park SY, Wu Z, Lee S, Kim S, and Liu KH (2021) In Vitro Metabolism of Donepezil in Liver Microsomes Using Non-Targeted Metabolomics. *Pharmaceutics* **13**:936.

Kiriyama A, Honbo A, Nishimura A, Shibata N, and Iga K (2016) Pharmacokinetic-pharmacodynamic analyses of antihypertensive drugs, nifedipine and propranolol, in spontaneously hypertensive rats to investigate characteristics of effect and side effects. *Regul Toxicol Pharmacol* **76**:21–29.

Kiriyama A, Kimura S, Banba C, Yamakawa M, Yajima R, Honbo A, and Iga K (2017) Pharmacokinetic-pharmacodynamic analyses of anti-diabetes, glimepiride: comparison of the streptozotocin-induced diabetic, GK, and Wistar rats. *J Drug Metab Toxicol* **8**:1000229.

Kobuchi S, Ito Y, Hayakawa T, Nishimura A, Shibata N, Takada K, and Sakaeda T (2014) Pharmacokinetic-pharmacodynamic (PK-PD) modeling and simulation of 5-fluorouracil for erythropenia in rats. *J Pharmacol Toxicol Methods* **70**:134–144.

Kobuchi S, Katsuyama Y, and Ito Y (2020) Mechanism-based pharmacokinetic-pharmacodynamic (PK-PD) modeling and simulation of oxaliplatin for hematological toxicity in rats. *Xenobiotica* **50**:223–230.

Kosasa T, Kuriya Y, Ogura H, and Yamanishi Y (1998) Effects of donepezil hydrochloride on the brain acetylcholine concentration in rats. *Jpn Pharmacol Ther* **26** (Suppl):s1303–s1311.

Kosasa T, Kuriya Y, and Yamanishi Y (1999) Effect of donepezil hydrochloride (E2020) on extracellular acetylcholine concentration in the cerebral cortex of rats. *Jpn J Pharmacol* **81**:216–222.

Matsui K, Mizuo H, Mishima M, Tadano K, Yoshimura T, Yuzuriha T, and Sato T (1998a) Absorption, Distribution, Metabolism, and Excretion of ^{14}C-Donepezil Hydrochloride after a Single Oral Administration to Beagle Dogs. *Jpn Pharmacol Ther* **26** (Suppl):s1357–s1371.

Matsui K, Kagei Y, Mizuo H, Mishima M, Tadano K, Yoshimura T, Yuzuriha T, and Sato T (1998b) Absorption, Distribution, Metabolism, and Excretion of ^{14}C-Donepezil Hydrochloride after a Single Oral Administration to Rats. *Jpn Pharmacol Ther* **26** (Suppl):s1339–s1355.

Matsui K, Mishima M, Nagai Y, Yuzuriha T, and Yoshimura T (1999a) Absorption, distribution, metabolism, and excretion of donepezil (Aricept) after a single oral administration to Rat. *Drug Metab Dispos* **27**:1406–1414.

Matsui K, Taniguchi S, and Yoshimura T (1999b) Correlation of the intrinsic clearance of donepezil (Aricept) between in vivo and in vitro studies in rat, dog and human. *Xenobiotica* **29**:1059–1072.

Matsui K, Taniguchi S, and Yoshimura T (2000) Identification of Cytochrome P450 Involved in the Metabolism of Donepezil and In Vitro Drug Interaction Study in Human Liver Microsome. *Xenobio Metabol Dispos* **15**:101–111.

Mishina M, Ohyama M, Ishii K, Kitamura S, Kimura Y, Oda K, Kawamura K, Sasaki T, Kobayashi S, Katayama Y et al. (2008) Low density of sigma1 receptors in early Alzheimer's disease. *Ann Nucl Med* **22**:151–156.

Motoki K, Igarashi T, Omura K, Nakatani H, Iwanaga T, Tamai I, and Ohashi T (2019) Pharmacokinetic/pharmacodynamic modeling and simulation of dotinurad, a novel uricosuric agent, in healthy volunteers. *Pharmacol Res Perspect* **7**:e00533.

Paxinos G and Watson C (1998) *The rat brain in stereotaxic coordinates*, Academic Press, San Diego.

Prvulovic D and Schneider B (2014) Pharmacokinetic and pharmacodynamic evaluation of donepezil for the treatment of Alzheimer's disease. *Expert Opin Drug Metab Toxicol* **10**:1039–1050.

Rogers SL and Friedhoff LT (1998a) Pharmacokinetic and pharmacodynamic profile of donepezil HCl following single oral doses. *Br J Clin Pharmacol* **46**(Suppl 1)1–6.

Rogers SL, Doody RS, Mohs RC, and Friedhoff LT; Donepezil Study Group (1998b) Donepezil improves cognition and global function in Alzheimer disease: a 15-week, double-blind, placebo-controlled study. *Arch Intern Med* **158**:1021–1031.

Sugimoto H, Yamanishi Y, Ogura H, Iimura Y, and Yamatsu K (1999) [Discovery and development of donepezil hydrochloride for the treatment of Alzheimer's disease]. *Yakugaku Zasshi* **119**:101–113.

Summers WK, Majovski LV, Marsh GM, Tachiki K, and Kling A (1986) Oral tetrahydroaminoacridine in long-term treatment of senile dementia, Alzheimer type. *N Engl J Med* **315**:1241–1245.

Takeuchi R, Shinozaki K, Nakanishi T, and Tamai I (2016) Local Drug-Drug Interaction of Donepezil with Cilostazol at Breast Cancer Resistance Protein (ABCG2) Increases Drug Accumulation in Heart. *Drug Metab Dispos* **44**:68–74.

Tanaka A, Koga S, and Hiramatsu Y (2009) Donepezil-induced adverse side effects of cardiac rhythm: 2 cases report of atrioventricular block and Torsade de Pointes. *Intern Med* **48**:1219–1223.

Tchedre KT and Yorio T (2008) sigma-1 receptors protect RGC-5 cells from apoptosis by regulating intracellular calcium, Bax levels, and caspase-3 activation. *Invest Ophthalmol Vis Sci* **49**:2577–2588.

Tiseo PJ, Perdomo CA, and Friedhoff LT (1998) Metabolism and elimination of 14C-donepezil in healthy volunteers: a single-dose study. *Br J Clin Pharmacol* **46**(Suppl 1)19–24.

van Waarde A, Ramakrishnan NK, Rybczynska AA, Elsinga PH, Ishiwata K, Nijholt IM, Luiten PG, and Dierckx RA (2011) The cholinergic system, sigma-1 receptors and cognition. *Behav Brain Res* **221**:543–554.

Watabe T, Naka S, Ikeda H, Horitsugi G, Kanai Y, Isohashi K, Ishibashi M, Kato H, Shimosegawa E, Watabe H et al. (2014) Distribution of intravenously administered acetylcholinesterase inhibitor and acetylcholinesterase activity in the adrenal gland: 11C-donepezil PET study in the normal rat. *PLoS One* **9**:e107427.

Whitehouse PJ, Price DL, Struble RG, Clark AW, Coyle JT, and Delon MR (1982) Alzheimer's disease and senile dementia: loss of neurons in the basal forebrain. *Science* **215**:1237–1239.

Yamanishi Y, Kosasa T, and Kuriya Y (1998a) Inhibitory effects of donepezil hydrochloride on cholinesterase activities in vitro. *Jpn Pharmacol Ther* **26** (Suppl):s1277–s1282.

Yamanishi Y, Kosasa T, Kuriya Y, Matsui K, and Kanai K (1998b) Inhibitory effects of donepezil hydrochloride on cholinesterase in brain, blood and peripheral tissues of young adult rats. -In comparison with aged rats-. *Jpn Pharmacol Ther* **26** (Suppl):s1295–s1302.

Yang S, Bhardwaj A, Cheng J, Alkayed NJ, Hurn PD, and Kirsch JR (2007) Sigma receptor agonists provide neuroprotection in vitro by preserving bcl-2. *Anesth Analg* **104**:1179–1184.

Yoon SK, Bae KS, Hong DH, Kim SS, Choi YK, and Lim HS (2020)Pharmacokinetic Evaluation by Modeling and Simulation Analysis of a Donepezil Patch Formulation in Healthy Male Volunteers. *Drug Des Devel Ther* **14**:1729–1737.

Address correspondence to: Akiko Kiriyama, Department of Pharmacokinetics, Faculty of Pharmaceutical Sciences, Doshisha Women's College of Liberal Arts, Kodo, Kyotanabe, Kyoto, 610-0395, Japan. E-mail address: akiriyam@dwc.doshisha.ac.jp